Received: 3 December 2025 | Revised: 3 May 2026 | Accepted: 20 May 2026

DOI: 10.1002/ame2.70245

ORIGINAL ARTICLE

A novel mouse model of chronic *Pseudomonas aeruginosa* infection inducing bronchiectasis-like phenotype

Heng Yang[1,2] | Yang Liu[1,2] | Yuqing Wang[1,2] | Yuhua Wen[2] | Yan Chen[2] | Rui Fan[2] | Jiayan Xu[2] | Shunlian Hu[1] | Hao Qian[1] | Rui Jiang[1] | Weijun Cao[2] | Jinfu Xu[1,2]

[1]Department of Respiratory and Critical Care Medicine, Tongji Hospital, School of Medicine, Tongji University, Shanghai, China

[2]Institute of Respiratory Medicine, Shanghai Pulmonary Hospital, School of Medicine, Tongji University, Shanghai, China

Correspondence
Jinfu Xu, Department of Respiratory and Critical Care Medicine, Tongji Hospital, School of Medicine, Tongji University, No. 389 Xincun Road, Shanghai 200065, China.
Email: jfxucn@163.com

Weijun Cao, Institute of Respiratory Medicine, Shanghai Pulmonary Hospital, School of Medicine, Tongji University, No. 507 Zhengmin Road, Shanghai 200433, China.
Email: weijuncao@126.com

Funding information
The Noncommunicable Chronic Diseases-National Science and Technology Major Project, Grant/Award Number: 2024ZD0522400; Natural Science Foundation of China, Grant/Award Number: 81925001 and 82330070; the Innovation Program of Shanghai Municipal Education Commission, Grant/Award Number: 202101070007-E00097; the Program of the Shanghai Municipal Science and Technology Commission, Grant/Award Number: 21DZ2201800; the Program of the Shanghai Shenkang Development Center, Grant/Award Number: SHDC12023110; the Major Project of Guangzhou National Laboratory, Grant/Award Number: GZNL2024A02003

Abstract

Background: Given the need to translate basic research into human therapies, the development and refinement of clinically relevant animal models for bronchiectasis are critically important. To date, there are no well-established animal models for bronchiectasis. Thus, our aim was to develop a novel animal model that accurately recapitulates bronchiectasis-like pathologies.

Methods: To address this question, clinical strains of chronic *Pseudomonas aeruginosa* (CPA) were embedded in agar beads in vitro; then CPA-loaded agar beads and papain were repeatedly instilled intratracheally in female C57BL/6J mice. Experimental assessments included micro-computed tomography (micro-CT) imaging, histological analysis, immune cell infiltration, cytokines, and lung function parameter measurements to evaluate structural damage, immune responses, and lung function impairments in the mouse model.

Results: In this mouse model, we observed that lung micro-CT imaging revealed significant bronchiectasis, with visible airways in the periphery, cylindrical airway expansion, and an airway-to-artery ratio >1. Histopathology highlighted immune cell infiltration around the trachea, including lymphocytes, neutrophils, and monocytes, along with Periodic acid–Schiff staining-positive hypermucinous secretion. Compared to controls, the bronchiectasis group exhibited elevated pro-inflammatory cytokines in bronchoalveolar lavage fluid and worse lung function.

Conclusion: Our study presented a novel mouse model that better replicated the bronchiectasis-like phenotype than the CPA airway infection model, showing the advantages of the "CPA-loaded agar beads and papain"–driven approach in optimizing the disease models. The model mimicked the progression of bronchiectasis closely and could be used for studies on disease pathogenesis as well as the evaluation of novel therapies in the near future.

Heng Yang, Yang Liu, and Yuqing Wang have contributed equally to this work.

KEYWORDS
bronchiectasis, micro-computed tomography (micro-CT), mouse model, *Pseudomonas aeruginosa*

1 | INTRODUCTION

Noncystic fibrosis bronchiectasis (hereafter referred to as bronchiectasis) is a chronic respiratory disease, causing a considerable burden on the healthcare system.[1,2] *Pseudomonas aeruginosa* represents the predominant micro-organism cultured from bronchiectatic airways, and its chronic pulmonary infection with *P. aeruginosa* is linked to higher rates of acute exacerbations as well as greater mortality among individuals with bronchiectasis.[3–5]

Knowledge of bronchiectasis pathophysiology has advanced considerably in recent decades, but we still lack a comprehensive understanding of disease progression.[6] Animal models have made significant contributions to elucidating specific mechanisms involved in clinical translational research.[7] Currently, the major obstacle in the study of bronchiectasis is the lack of suitable disease animal models that accurately recapitulate bronchiectasis-like phenotype. Establishing murine models that accurately replicate chronic *P. aeruginosa* (CPA) airway infection remains difficult, because introducing free-living *P. aeruginosa* into mice typically results in either fulminant sepsis with early mortality or rapid clearance, preventing long-term colonization.[8] At present there is no established animal model for bronchiectasis, which is usually replaced by using the *P. aeruginosa* agar-beads mouse model. However, this chronic infection model primarily focuses on studying the pulmonary inflammation and infection associated with the disease, but it has limitations in replicating typical bronchiectasis-like radiological features, thereby restricting its application in the study of bronchiectasis-related pathological mechanisms and therapeutic interventions.[9,10]

We recently developed an improved mouse infection model for bronchiectasis by focusing primarily on "CPA-loaded agar beads and papain"–driven approach. In this study, we detailed the methodology for using a combination of CPA strain-loaded agar beads and papain, which were repeatedly instilled intratracheally in mice. Subsequent evaluations included micro-computed tomography (micro-CT) imaging, histological staining, immune cell infiltration, inflammatory cytokine, and lung function assessments in mice. Overall, we established a novel mouse model that mimicked most of the pathological features of human bronchiectasis. The mouse model will assist researchers in addressing fundamental questions regarding the pathogenesis of bronchiectasis and provide technical support for the development of novel therapies for the disease.

2 | METHODS

2.1 | Animals

Female C57BL/6J mice (~18 g, 6 weeks old) were procured from Shanghai SLRC Laboratory Animal Center.

2.2 | Preparation of CPA-loaded agar beads

It mainly refers to the methodology of Professor Alessandra Bragonzi.[10]

1. Preparation of bacteria
   a. Pick a single colony of the CPA strain and inoculate it into a sterile shaking tube containing 4 mL of Luria–Bertani (LB) medium. Culture at 37°C with shaking at 220 rpm for 16–18 h. The CPA strain was originally isolated from a bronchiectasis patient.
   b. Transfer 500 μL of the initially shaken bacterial solution into a sterile 50 mL centrifuge tube containing a final volume of 10 mL, and prepare two identical aliquots. Place these mixtures in the incubator at 37°C, with shaking at 220 rpm for 4–5 h. Isolate bacterial cells via centrifugation at 2700 *g* for 3 min at 4°C, and then reconstitute the bacterial pellet in 1 mL of the supernatant.
2. Embedding bacteria in agar beads
   a. Preheat 150 mL of paraffin liquid (MACKLIN, catalog no. C16090135) in a 250 mL Erlenmeyer flask, maintaining a constant temperature of 50°C. Additionally, prepare LB medium containing 1.5% agar at a temperature not exceeding 60°C.
   b. Add 1 mL of bacterial suspension to 10 mL of LB medium with 1.5% agar, and mix thoroughly. Transfer the 10 mL LB–CPA strain mixture into paraffin liquid and stir for 6 min at 2000 rpm.
   c. Mix slowly for 35 min at 4°C; then allow it to settle on ice for 20 min.
   d. Transfer the agar beads into 50 mL centrifuge tubes and centrifuge.
   e. Discard the paraffin liquid thoroughly, and add phosphate-buffered saline (PBS) to resuspend.
   f. Discard ~10 mL of the oil-containing PBS, aspirate the solution of smaller beads, and discard the lower layer containing larger particle beads.
   g. Filter the beads obtained in the previous step through 200- and 100-μm filters to obtain beads with a diameter of 100–200 μm, with a final volume of ~5–15 mL. Finally, perform bacterium colony counting.

2.3 | Mouse challenge with CPA-loaded agar beads and papain

The animals were anesthetized, and either 30 μL of CPA-loaded agar beads containing 3×10^6 colony-forming units or 20 μL of 1.25 mg/mL papain was administered (Sangon Biotech, CAS number 9001-73-4). This procedure was carried out once a week for 4 weeks

(the framework is shown in Figure 1). The beads were usable up to 1 month at 4°C. During the second, third, and fourth modeling sessions, beads or papain was administered slowly to avoid mouse mortality due to respiratory depression.

2.4 | Micro-computed tomography

The mouse was positioned on the imaging platform carefully. The mouse was placed in a prone position, with its body aligned symmetrically to the axis of the scanner to ensure optimal image acquisition. Scanning procedure: the scan was performed by selecting the appropriate imaging protocol. High-resolution scanning was performed using the Quantum GX2 CT scanner (PerkinElmer), with parameters set to 90 kV and 88 mA.

2.5 | Histological examination

The lobes of the left lung of mice were removed and fixed in 4% formaldehyde. After processing, the tissue samples were stained using two techniques: hematoxylin and eosin (H&E) staining for general histopathological evaluation of lung damage, and Periodic acid–Schiff (PAS) staining for detecting carbohydrate-rich components, such as PAS-positive goblet cells or mucus, using a PAS staining kit.[11]

2.6 | Lung function measurement

Before initiating the experiment, both the airflow sensor and the amplifier must be calibrated to ensure accurate measurements, following

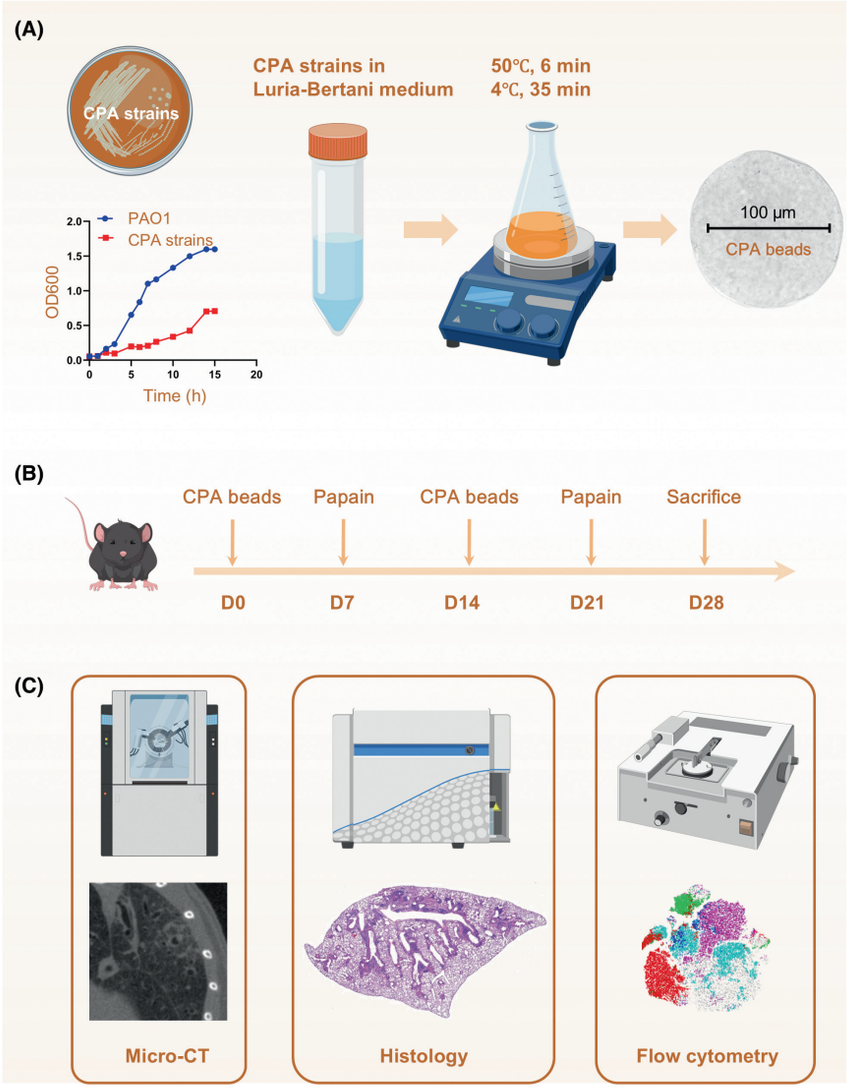

FIGURE 1 Schematic diagram of the bronchiectasis mouse model construction. (A) Preparation of chronic *Pseudomonas aeruginosa* (CPA)-loaded agar beads. CPA-loaded agar beads were carefully prepared to achieve persistent infections. (B) Mice were challenged to CPA-loaded agar beads in combination with papain to produce the bronchiectasis mouse model. (C) The primary experimental methods employed in this study include micro-computed tomography (micro-CT), histological analysis, and flow cytometry. Created using BioGDP.com.

the instrument's guidelines (Harvard Apparatus, catalog no. 55-7040). The mice were anesthetized to induce controlled sedation. After anesthesia, a tracheostomy was performed using the FTC102 tracheal cannula to establish an airway access. The mice received ventilation at 200 μL of tidal volume and 150 breaths/min. Data recording was initiated to capture the relevant respiratory parameters.

Detailed methods for flow cytometry and enzyme-linked immunosorbent assay (ELISA) are provided in the supplementary material.

2.7 | Statistical analysis

We performed statistical analysis using GraphPad Prism, version 9.2. For comparing the two groups, we employed a two-sided unpaired *t*-test when the data followed a normal distribution and a two-sided Mann–Whitney *U*-test for nonnormal data distributions. Statistical significance was established at a threshold of $p < 0.05$. All measurements were obtained from independent samples, and each experiment was repeated three to five times.

3 | RESULTS

3.1 | CPA-loaded agar bead and papain challenge induces a typical bronchiectasis-like radiological phenotype in the mouse model

In this study, we utilized mouse pulmonary micro-CT imaging to confirm whether the developed mouse model exhibited bronchiectasis-like radiological features. The diagnostic criteria were based on the standard radiological definitions used in bronchiectasis adults.[12,13] Mice treated with CPA-loaded agar

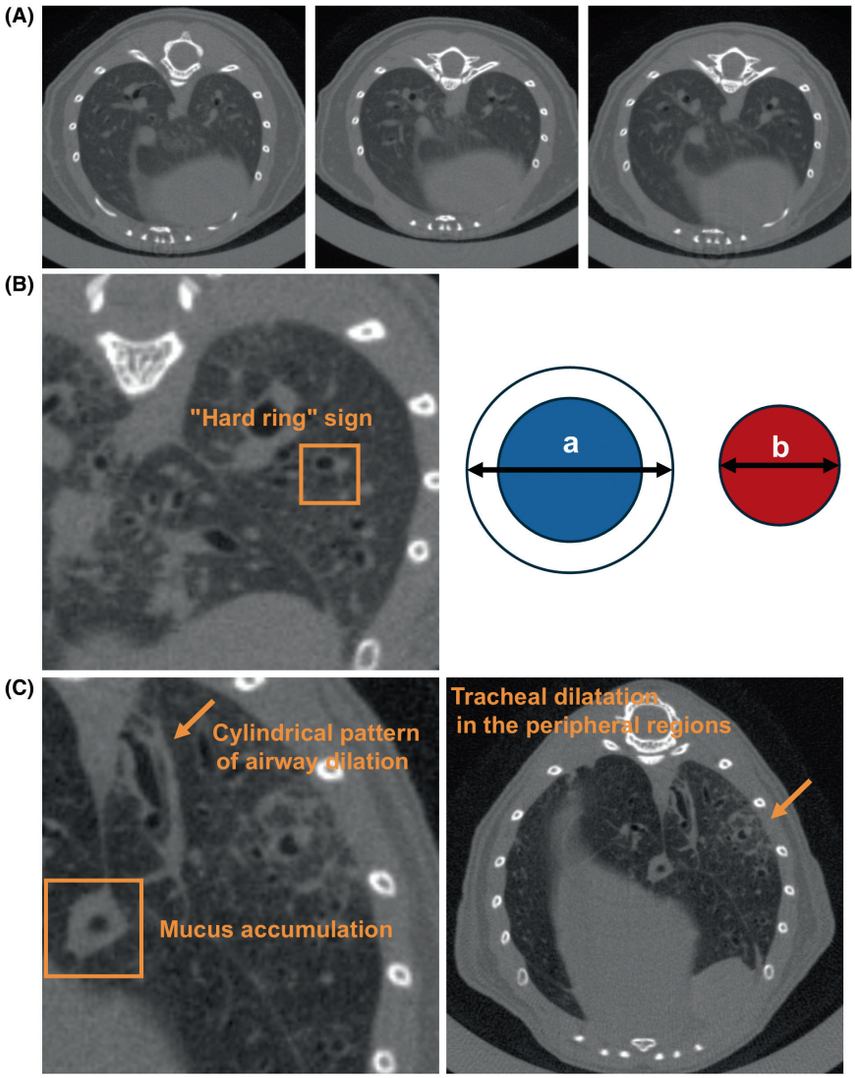

FIGURE 2 CPA (chronic *Pseudomonas aeruginosa*)–loaded agar beads and papain challenge induces a typical bronchiectasis-like phenotype in the mouse model. (A) Representative micro-CT (micro-computed tomography) images of control mouse lungs. (B) Axial micro-CT image (left) and schematic drawing (right) showing the dimensions of the trachea and accompanying vessels. (C) The radiological findings included cylindrical airway dilatation, increased visibility of airways in the periphery, and mucous accumulation.

beads alone for 28 days exhibited only mild peribronchial inflammatory changes in micro-CT imaging, and no typical bronchiectasis-like lesions were observed (Figure S1). In contrast, longitudinal micro-CT imaging of the bronchiectasis model group revealed a time-dependent progression of bronchiectasis-like changes (Figure S2A). At day 14 postinduction, only mild airway dilatation was observed, whereas by day 28, the extent of airway dilatation significantly increased (Figure S2B). Particularly, the number of peripheral signet ring signs was substantially higher in the 28-day group (Figure S2C), indicating more advanced structural distortion of the airways. These findings suggest that airway injury and remodeling peaked at ~day 28, which was therefore selected as the optimal time point for subsequent experiments. Representative micro-CT images of the lungs from control mice are shown in Figure 2A, where clear lung markings are observed without any signs of bronchiectasis. In contrast, the bronchiectasis model group exhibited typical bronchiectasis-like radiological features (Figure 2B,C) First, as shown in Figure 2B, the inner airway-to-artery diameter ratio was measured as 0.42 mm/0.23 mm, 0.38 mm/0.24 mm, and 0.39 mm/0.22 mm (Figure 3A) in the bronchiectasis group. All these ratios exceeded 1, meeting the diagnostic criterion for bronchiectasis. Additionally, the typical signet ring sign was evident in all cases, further enhancing diagnostic reliability. Second, a cylindrical pattern of airway expansion was observed in the bronchiectasis model group (Figures 2C and 3B), characterized by the absence of normal tapering in the distal airways, along with increased mucous accumulation (Figure 2C). Third, the CT images revealed visible airways in the periphery of the lungs, a characteristic feature of bronchiectasis (Figures 2C and 3C). These three distinct imaging characteristics provided the strongest basis for the radiological diagnosis of bronchiectasis.

3.2 | Bronchiectasis-like pathological phenotypes in mouse model

Histological examination of H&E-stained sections revealed intact lung structure in the control group, with no significant infiltration of inflammatory cells (Figures 4A and S3). Mice in the 14-day group exhibited variable and relatively mild airway inflammatory changes (Figure S3). The bronchiectasis group exhibited mild pulmonary inflammation, with the inflammatory areas mainly distributed around the airways (Figure 4B,C), which differed from the extensive lung damage typically observed in acute infection and severe lung injury. Moreover, histopathological examination revealed that the trachea was predominantly surrounded by lymphocytes, neutrophils, and monocytes, indicating an active immune

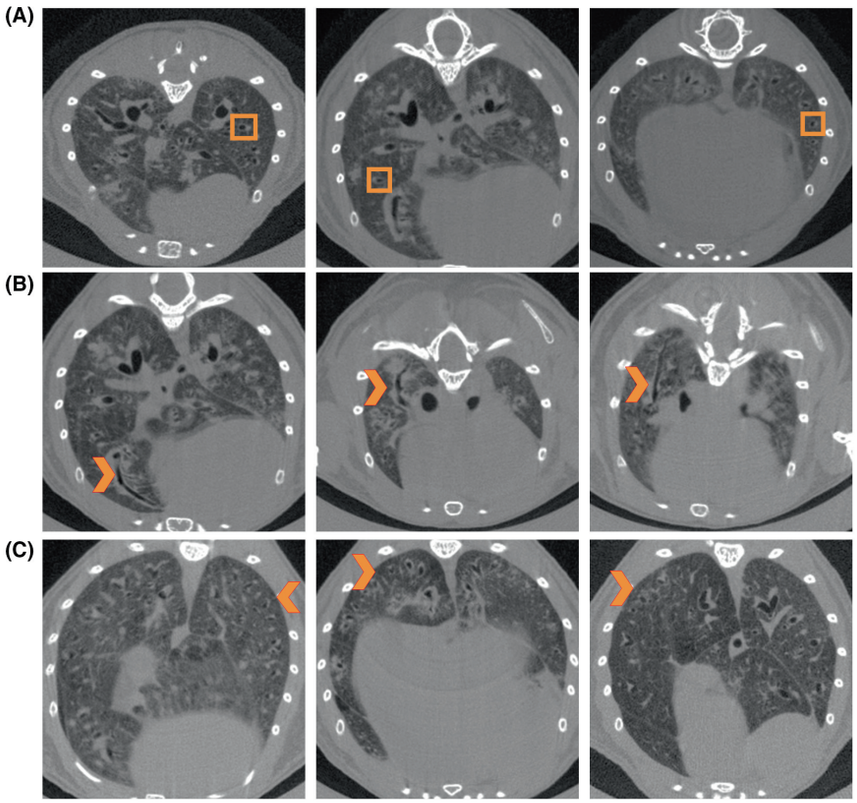

FIGURE 3 Representative micro-CT (micro-computed tomography) images highlighting bronchiectasis radiological features in the mouse model. (A) Micro-CT images showing the signet ring sign, characterized by airway diameters of 0.42 mm/0.23 mm, 0.38 mm/0.24 mm, and 0.39 mm/0.22 mm, respectively. (B) Micro-CT images demonstrating the absence of normal airway tapering. (C) Micro-CT images showing the visibility of airways extending to the periphery of lungs.

response around the airways. Additionally, pronounced infiltration of inflammatory cells was observed around the blood vessels, with lesions predominantly concentrated in the central regions of the lung.

To further investigate airway mucous secretion, PAS staining was performed, with positive results indicating increased mucous secretion. In our study, we did not observe significant PAS-positive regions in the normal group (Figure 5A). In contrast, the bronchiectasis group exhibited more PAS-positive areas, indicating excessive mucous secretion (Figure 5B,C).

3.3 | Pulmonary immune response characteristics in the bronchiectasis mouse model

To gain a comprehensive understanding of host immune function in bronchiectasis, we conducted fluorescence-activated cell sorting-assisted immunophenotyping of $CD45^+$ infiltrates in mouse lungs. In the bronchiectasis mouse model, most myeloid cell populations, such as neutrophils, interstitial macrophages, conventional dendritic cells, and eosinophils, increased (Figures 6A and S5). Additionally, the pulmonary immune response mediated by lymphocytes was characterized by an increase in cytotoxic cell populations, such as natural killer (NK) cells, whereas the proportion of B cells decreased (Figures 6B and S6).

3.4 | Elevated pro-inflammatory cytokines and worse lung function were observed in the bronchiectasis mouse model

Mice in the bronchiectasis group exhibited a significant reduction in body weight (Figure 7A). Additionally, the bronchiectasis group exhibited a significant increase in airway resistance average (RI, $cmH_2O/mL/s$) and a significant decrease in the dynamic compliance of the lung (CDyn, mL/cmH_2O) (Figure 7B,C). Furthermore, the bronchiectasis group's bronchoalveolar lavage fluid (BALF) exhibited significantly higher levels of pro-inflammatory cytokines, including tumor necrosis factor-α (TNF-α) and interleukin-6 (Figure 7D–F).

4 | DISCUSSION

For bronchiectasis, one of the main challenges in studying the interaction between the host and colonizing bacteria is selecting an appropriate animal model to address disease-related questions. Animal models are

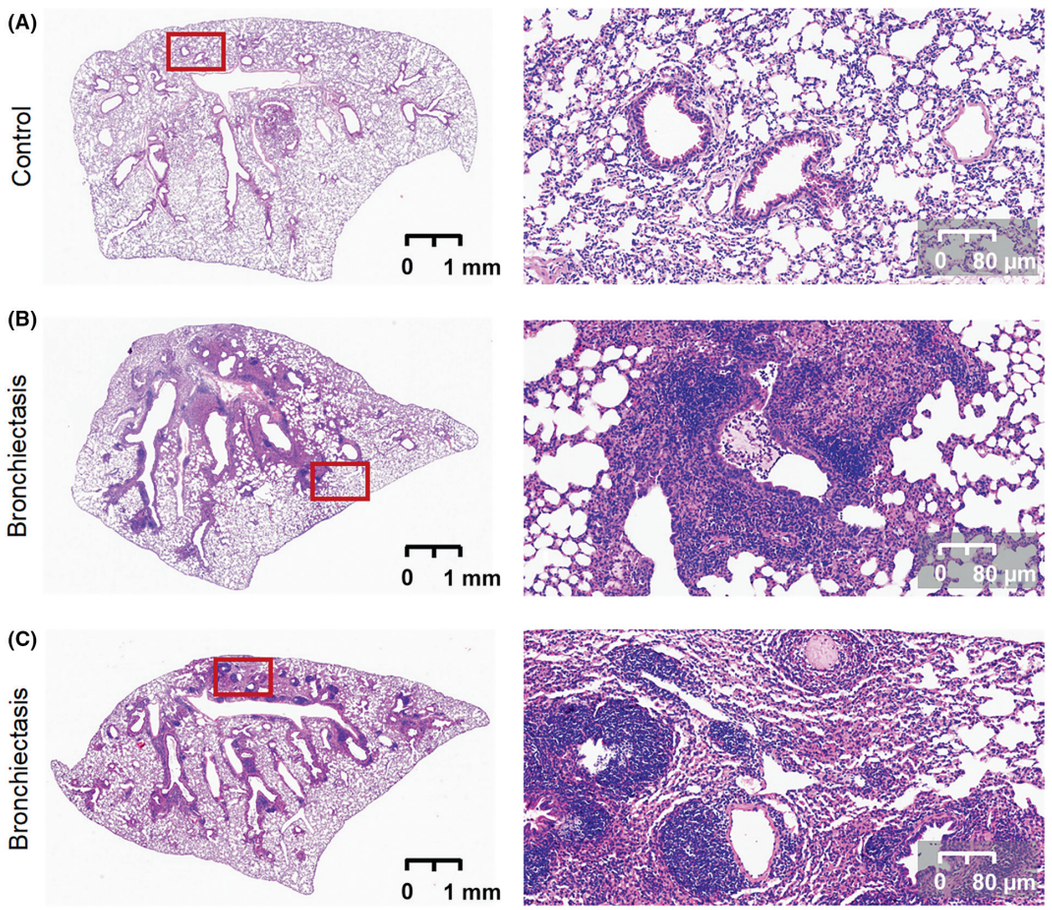

FIGURE 4 Hematoxylin and eosin (H&E) staining of lung tissue sections in the bronchiectasis mouse model. (A) H&E staining of lung tissue from control mice. (B, C) H&E staining of lung tissue from bronchiectasis mice, exhibiting bronchiectasis-like pathological changes.

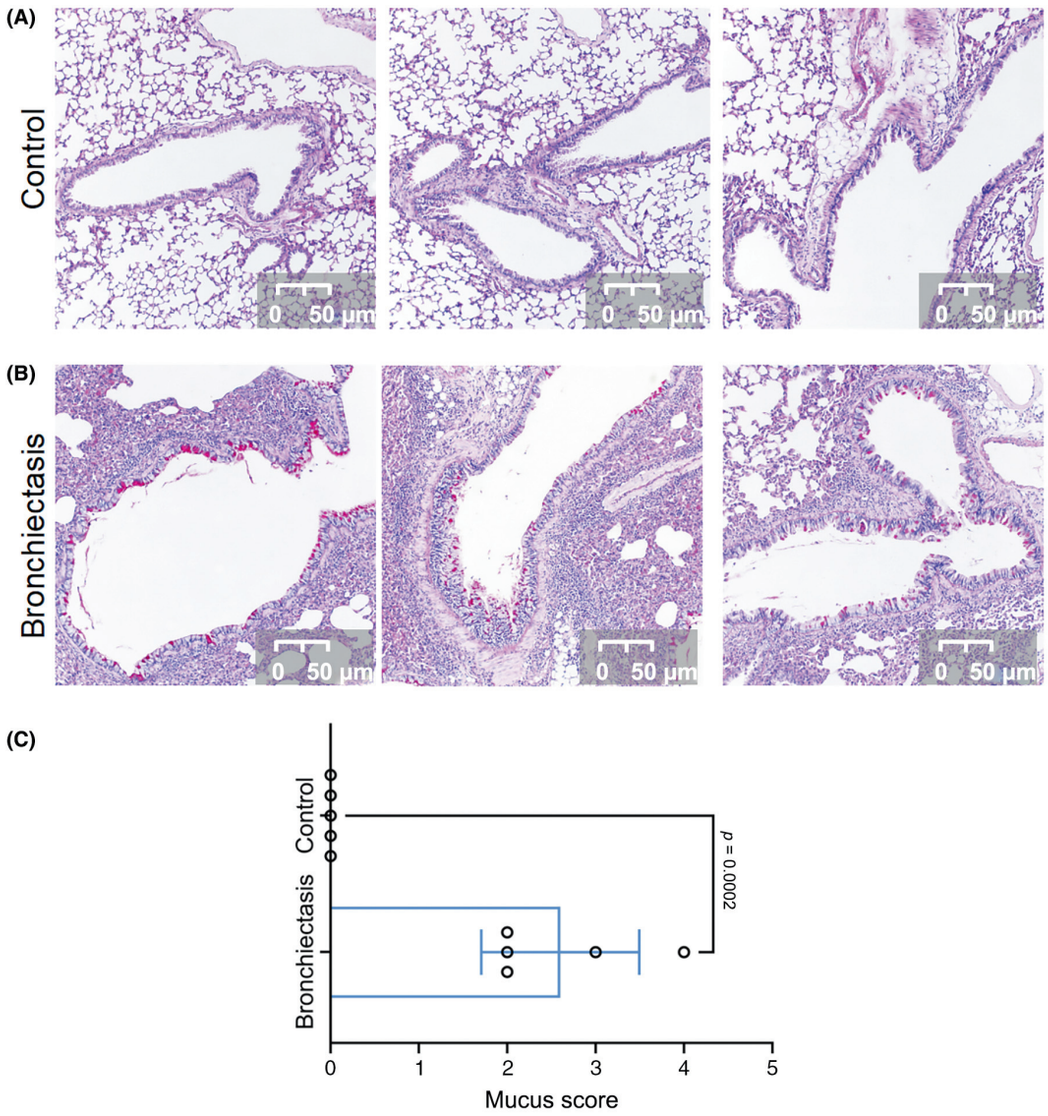

FIGURE 5 PAS (Periodic acid–Schiff) staining of lung tissue in the bronchiectasis mouse model. (A) PAS-stained sections of lung tissue from control mice. (B) PAS-stained sections from the bronchiectasis mouse model, demonstrating enhanced mucin secretion. (C) Quantification of goblet cell hyperplasia scores ($n = 5$ per group). Data are presented as mean ± SEM (standard error of the mean).

indispensable for transforming fundamental scientific discoveries into clinical practice.[14] To enhance the clinical relevance of animal models, scientists focused on simulating the pathological features of pathogens within the host to increase their similarity to human diseases.[15] This was a crucial aspect in the development of the disease models, as the behavior of pathogens within the host directly influences the host's immune response and its reaction to clinical interventions.[7] In this study, we developed an innovative animal model aimed at mimicking *P. aeruginosa* airway infection in bronchiectasis, with the aim of replicating the pulmonary pathological features of the disease more accurately. In the past, there was no suitable animal model for bronchiectasis. Researchers typically employed CPA airway infection models, which primarily focused on the pathological processes of chronic airway infection and inflammation but lacked the characteristic of bronchiectasis-like radiological phenotype, thus limiting research on the underlying mechanisms of bronchiectasis and the development of novel therapeutic interventions.

This study was the first to develop an animal model capable of reproducing the pulmonary pathological features of human bronchiectasis using the "CPA-loaded agar beads and papain"–driven approach. The addition of papain not only reduced the mortality rate of the mice but also caused structural changes in the airways (Figure S4). Papain was primarily used to model emphysema in rats.[16] Given the differences in pulmonary pathology between emphysema and bronchiectasis, we continuously refined our model protocol by reducing the concentration of papain to minimize its penetration into the alveoli and subsequent alveolar damage. Besides, preexisting airway pathology alters protease distribution. In our model, CPA-loaded agar beads were instilled before papain, inducing localized infectious and inflammatory foci predominantly around bronchi. Additionally, to enhance infection efficiency when constructing the animal model with CPA-coated agar beads, mice were temporarily suspended.

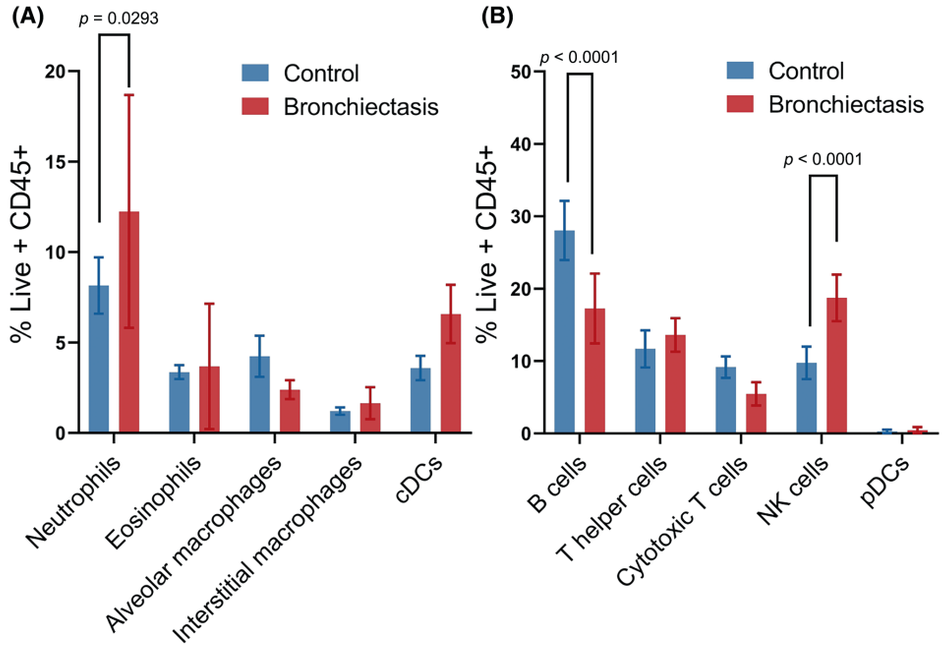

FIGURE 6 Immune cell infiltration in the lungs of the bronchiectasis mouse model. (A) Bar chart showing the percentage of all myeloid cell subsets in both groups of mice. (B) Bar chart showing the percentage of all lymphoid cell subsets in both groups of mice ($n = 5$ for the control group, $n = 7$ for the bronchiectasis group).

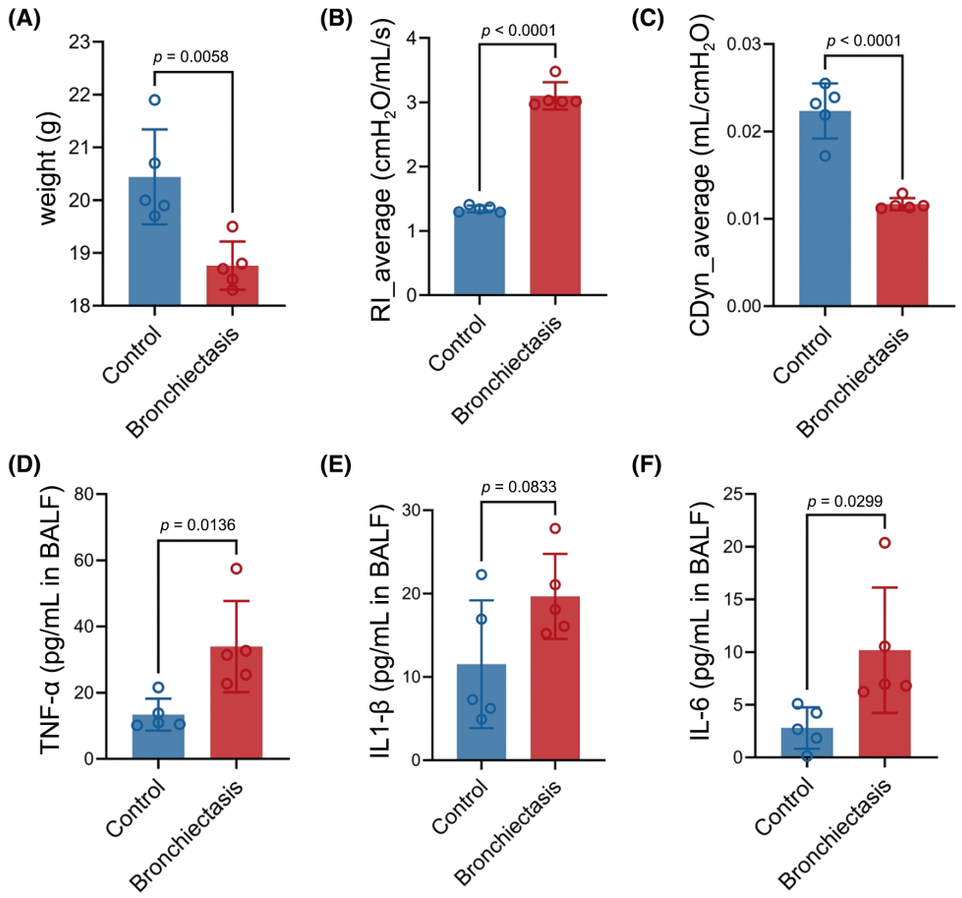

FIGURE 7 Systemic inflammatory state and lung function changes in the bronchiectasis mouse model. (A) Comparison of body weight between control and bronchiectasis mouse model groups. (B, C) Comparison of airway resistance and lung compliance between the two groups of mice. (D–F) Difference in inflammatory cytokine levels in BALF from both groups of mice ($n = 5$ per group).

Conversely, after papain stimulation, mice were immediately placed in a prone position to reduce the delivery of papain to the distal airways and the resultant changes in alveolar structure, all of which, both physically and biochemically, remains largely confined to the proximal airways in terms of papain activity.

Micro-CT imaging and hispathological analysis of the model showed mild emphysema-like changes. After 28 days of modeling, micro-CT scans showed typical bronchiectasis-like radiological features in both lungs of the mouse model, including an airway-to-artery diameter ratio (either inner or outer) ≥1.0, the absence of airway tapering, and visible airways in the periphery of the lungs. These meet the criteria for the radiological diagnosis of adult bronchiectasis as defined by current international guidelines.[13] Therefore, the 28-day modeling protocol was selected as the optimal timeline for inducing bronchiectasis.

Furthermore, in the bronchiectasis mouse model, the integrity of the lung barrier was compromised, and significant infiltration of various immune cells was observed, as evidenced by histopathological analysis. The proportion of neutrophils and eosinophils significantly increased, which ultimately led to excessive mucous secretion in the airways.[11,17] This impairment was confirmed by PAS staining, which showed an increase in PAS-positive cells, further validating the strong potential of this animal model to replicate bronchiectasis.

CPA airway infection led to sustained immune responses in the host, particularly those mediated by innate immune cells.[18] Our animal model demonstrated a neutrophil increase in the bronchiectasis group, along with a decrease in AMs and a trend toward an increase in eosinophils. In bronchiectasis, heightened concentrations of pro-inflammatory mediators and neutrophil serine proteases promote the recruitment of neutrophils to the airways.[19] Besides, eosinophils are recognized for their pro-inflammatory activity and their role in promoting airway remodeling and injury.[20] These aligned with the typical neutrophil-driven airway inflammation observed in our model, as well as the increased eosinophils. Alveolar macrophages (AMs) or interstitial macrophages consist of subpopulations with distinct transcriptional profiles that either promote or suppress inflammation in a highly regulated and coordinated manner.[21] AMs often undergo cell death upon pathogen exposure, and the fragments produced due to their death could activate multiple immune cell types, thus initiating a feedforward amplification of the inflammation response.[22,23] Interestingly, in the bronchiectasis mouse model, NK cells substantially increase in proportion. NK cells circulate innate lymphocytes that play important roles in host defense by directly killing bacteria or infected cells and producing important cytokines.[24] Patients with NK cell deficiencies are more prone to invasive bacterial infection, bacterial sepsis, and bacterial pneumonia.[25] Furthermore, NK cells could promote neutrophil survival and function as essential mediators linking innate and adaptive immunity during lung infection.[26] The immune cell alterations in the bronchiectasis mouse model closely resembled the immunological features observed in the lungs of bronchiectasis patients, further confirming the reliability of the animal model.

In our study, the mice in the bronchiectasis group exhibited significant weight loss. Bronchiectasis patients may present with underweight and/or malnutrition, which impacts lung function, immune function, physical function, and strength. The study showed that being underweight was associated with increased mortality in bronchiectasis.[27,28] This aligned with our bronchiectasis animal model. Lung function in bronchiectasis usually leads to an obstructive defect. The mechanisms are not fully known but possibly involve the collapse of large airways, bronchial wall thickening, and mucus retention.[29] Similarly, the pulmonary function tests in our mouse model indicated compromised lung tissue elasticity and compliance, primarily manifested as small airway dysfunction. These findings strongly supported the ability of our mouse model to closely mimic the clinical features of bronchiectasis.

Several important limitations should be considered in our study. First, mouse size constrained the spatial resolution of micro-CT imaging. Second, the use of only female mice may affect the generalizability of findings due to known sex differences in immune responses. Third, we did not directly assess mucociliary clearance function. Finally, repeated anesthesia and tracheal procedures could represent potential confounding factors. Importantly, these acknowledged limitations did not compromise the core radiological or pathological characterization of the model. In future research, extending this work to larger animal models may allow for higher-resolution imaging and provide an opportunity to address these functional and confirmatory endpoints in a more comprehensive manner.

In conclusion, developing animal models that mimic bronchiectasis is challenging, particularly mouse models. Our findings demonstrated the efficacy of the "CPA-loaded agar beads and papain"–driven approach in establishing a novel mouse model that mimics most of the human bronchiectasis characteristics. We anticipate the model will serve extensively in disease mechanism research and therapeutic assessment.

AUTHOR CONTRIBUTIONS

Jinfu Xu: Conceptualization; funding acquisition; project administration. **Weijun Cao:** Conceptualization; project administration. **Heng Yang:** Formal analysis; investigation; methodology; writing – original draft. **Yang Liu:** Data curation; formal analysis; methodology; validation; writing – original draft. **Yuqing Wang:** Methodology; validation; writing – review and editing. **Yuhua Wen:** Data curation. **Yan Chen:** Data curation. **Rui Fan:** Resources; writing – review and editing. **Jiayan Xu:** Resources; writing – review and editing. **Shunlian Hu:** Methodology. **Hao Qian:** Methodology. **Rui Jiang:** Methodology.

ACKNOWLEDGMENTS

We sincerely thank Professor Hexige Saiyin for his invaluable contributions and technical support with micro-CT imaging.

FUNDING INFORMATION

This work was supported by the Noncommunicable Chronic Diseases-National Science and Technology Major Project (2024ZD0522400), the National Natural Science Foundation of China (81925001, 82330070),

the Innovation Program of Shanghai Municipal Education Commission (202101070007-E00097), the Program of the Shanghai Municipal Science and Technology Commission (21DZ2201800); the Program of the Shanghai Shenkang Development Center (SHDC12023110), and the Major Project of Guangzhou National Laboratory (Grant no. GZNL2024A02003).

CONFLICT OF INTEREST STATEMENT

All authors declare no conflict of interest that may directly or indirectly influence the content of the manuscript submitted.

DATA AVAILABILITY STATEMENT

The data that support the findings of this study are available from the corresponding author upon reasonable request.

ETHICS STATEMENT

All animal experiments were approved by the Institutional Animal Care and Use Committee of Tongji University (TJBE00122105).

PATIENT CONSENT STATEMENT

This study did not involve human participants.

PERMISSION TO REPRODUCE MATERIAL FROM OTHER SOURCES

No permissions are required. All content is original.

CLINICAL TRIAL REGISTRATION

This study did not involve clinical trial.

ORCID

Jin-Fu Xu https://orcid.org/0000-0002-8039-8973

REFERENCES

1. Choi H, Yang B, Nam H, et al. Population-based prevalence of bronchiectasis and associated comorbidities in South Korea. *Eur Respir J*. 2019;54(2):1900194. doi:10.1183/13993003.00194-2019
2. Dean SG, Blakney RA, Ricotta EE, et al. Bronchiectasis-associated infections and outcomes in a large, geographically diverse electronic health record cohort in the United States. *BMC Pulm Med*. 2024;24(1):172. doi:10.1186/s12890-024-02973-3
3. Haworth CS, Shteinberg M, Winthrop K, et al. Inhaled colistimethate sodium in patients with bronchiectasis and *P. aeruginosa* infection: results of PROMIS-I and PROMIS-II, two randomised, double-blind, placebo-controlled phase 3 trials assessing safety and efficacy over 12 months. *Lancet Respir Med*. 2024;12(10):787-798. doi:10.1016/S2213-2600(24)00225-X
4. Luo R, Miao X, Luo L, Mao B, Yu F, Xu J. Presence of pldA and exoU in mucoid *Pseudomonas aeruginosa* is associated with high risk of exacerbations in non-cystic fibrosis bronchiectasis patients. *Clin Microbiol Infect*. 2019;25(5):601-606. doi:10.1016/j.cmi.2018.07.008
5. Chai Y, Xu J. How does *Pseudomonas aeruginosa* affect the progression of bronchiectasis? *Clin Microbiol Infect*. 2020;26(3):313-318. doi:10.1016/j.cmi.2019.07.010
6. Long MB, Chotirmall SH, Shteinberg M, Chalmers JD. Rethinking bronchiectasis as an inflammatory disease. *Lancet Respir Med*. 2024;12(11):901-914. doi:10.1016/S2213-2600(24)00176-0
7. Duncan RP, Moustafa DA, Lewin GR, et al. Improvement of a mouse infection model to capture *Pseudomonas aeruginosa* chronic physiology in cystic fibrosis. *Proc Natl Acad Sci USA*. 2024;121(33):e2406234121. doi:10.1073/pnas.2406234121
8. Reyne N, McCarron A, Cmielewski P, Parsons D, Donnelley M. To bead or not to bead: a review of *Pseudomonas aeruginosa* lung infection models for cystic fibrosis. *Front Physiol*. 2023;14:1104856. doi:10.3389/fphys.2023.1104856
9. van Heeckeren AM, Schluchter MD. Murine models of chronic *Pseudomonas aeruginosa* lung infection. *Lab Anim*. 2002;36(3):291-312. doi:10.1258/002367702320162405
10. Facchini M, De Fino I, Riva C, Bragonzi A. Long term chronic *Pseudomonas aeruginosa* airway infection in mice. *J Vis Exp*. 2014;85:51019. doi:10.3791/51019
11. Hao Y, Kuang Z, Walling BE, et al. *Pseudomonas aeruginosa* pyocyanin causes airway goblet cell hyperplasia and metaplasia and mucus hypersecretion by inactivating the transcriptional factor FoxA2. *Cell Microbiol*. 2012;14(3):401-415. doi:10.1111/j.1462-5822.2011.01727.x
12. Meerburg JJ, Veerman GDM, Aliberti S, Tiddens HAWM. Diagnosis and quantification of bronchiectasis using computed tomography or magnetic resonance imaging: a systematic review. *Respir Med*. 2020;170:105954. doi:10.1016/j.rmed.2020.105954
13. Aliberti S, Goeminne PC, O'Donnell AE, et al. Criteria and definitions for the radiological and clinical diagnosis of bronchiectasis in adults for use in clinical trials: international consensus recommendations. *Lancet Respir Med*. 2022;10(3):298-306. doi:10.1016/S2213-2600(21)00277-0
14. Barré-Sinoussi F, Montagutelli X. Animal models are essential to biological research: issues and perspectives. *Future Sci OA*. 2015;1(4):FSO63. doi:10.4155/fso.15.63
15. Thomsen K, Kobayashi O, Kishi K, et al. Animal models of chronic and recurrent *Pseudomonas aeruginosa* lung infection: significance of macrolide treatment. *APMIS*. 2022;130(7):458-476. doi:10.1111/apm.13161
16. Gross P, Pfitzer EA, Tolker E, Babyak MA, Kaschak M. Experimental emphysema: its production with papain in normal and silicotic rats. *Arch Environ Health*. 1965;11:50-58. doi:10.1080/00039896.1965.10664169
17. Hayashi R, Srisomboon Y, Iijima K, et al. Cholinergic sensing of allergen exposure by airway epithelium promotes type 2 immunity in the lungs. *J Allergy Clin Immunol*. 2024;153(3):793-808. doi:10.1016/j.jaci.2023.10.031
18. Lambrecht BN. Alveolar macrophage in the driver's seat. *Immunity*. 2006;24(4):366-368. doi:10.1016/j.immuni.2006.03.008
19. Keir HR, Shoemark A, Huang JTJ, Chalmers JD. SPLUNC1 is a novel marker of disease severity and airway infection in bronchiectasis. *Eur Respir J*. 2021;58(5):2101840. doi:10.1183/13993003.01840-2021
20. Campisi R, Nolasco S, Mancuso M, et al. Eosinophilic bronchiectasis: prevalence, severity, and associated features-a cohort study. *J Clin Med*. 2024;13(16):4932. doi:10.3390/jcm13164932
21. Hoyer FF, Naxerova K, Schloss MJ, et al. Tissue-specific macrophage responses to remote injury impact the outcome of subsequent local immune challenge. *Immunity*. 2019;51(5):899-914. doi:10.1016/j.immuni.2019.10.010
22. Dagvadorj J, Shimada K, Chen S, et al. Lipopolysaccharide induces alveolar macrophage necrosis via cd14 and the p2x7 receptor leading to interleukin-1α release. *Immunity*. 2015;42:640-653. doi:10.1016/j.immuni.2015.03.007
23. Cai B, Thorp EB, Doran AC, et al. MerTK receptor cleavage promotes plaque necrosis and defective resolution in atherosclerosis. *J Clin Invest*. 2017;127(2):564-568. doi:10.1172/JCI90520
24. Louis C, Souza-Fonseca-Guimaraes F, Yang Y, et al. NK cell-derived GM-CSF potentiates inflammatory arthritis and is negatively regulated by CIS. *J Exp Med*. 2020;217(5):e20191421. doi:10.1084/jem.20191421

25. Ebbo M, Gérard L, Carpentier S, et al. Low circulating natural killer cell counts are associated with severe disease in patients with common variable immunodeficiency. *EBioMedicine*. 2016;6:222-230. doi:10.1016/j.ebiom.2016.02.025
26. McDonnell MJ, Anwar GA, Rutherford RM, et al. Lack of association between KIR and HLA-C type and susceptibility to idiopathic bronchiectasis. *Respir Med*. 2014;108(8):1127-1133. doi:10.1016/j.rmed.2014.05.017
27. Yang B, Han K, Kim SH, et al. Being underweight increases the risk of non-cystic fibrosis bronchiectasis in the young population: a nationwide population-based study. *Nutrients*. 2021;13(9):3206. doi:10.3390/nu13093206
28. Lee JM, Lee SA, Han CH, et al. Body mass index as a predictor of mortality in bronchiectasis: a nationwide population-based study. *Respir Med*. 2021;180:106370. doi:10.1016/j.rmed.2021.106370
29. Lopes AJ, Camilo GB, de Menezes SLS, Guimarães FS. Impact of different etiologies of bronchiectasis on the pulmonary function tests. *Clin Med Res*. 2015;13(1):12-19. doi:10.3121/cmr.2014.1236

SUPPORTING INFORMATION

Additional supporting information can be found online in the Supporting Information section at the end of this article.

How to cite this article: Yang H, Liu Y, Wang Y, et al. A novel mouse model of chronic *Pseudomonas aeruginosa* infection inducing bronchiectasis-like phenotype. *Anim Models Exp Med*. 2026;9:1409-1419. doi:10.1002/ame2.70245